Journal of Machine Engineering, 2018, Vol. 18, No. 1, 95-106
ISSN 1895-7595 (Print) ISSN 2391-8071 (Online)

Received: *27 December 2017* / Accepted: *12 February 2018* / Published online: *12 March 2018*

additive manufacturing, part decomposition, multi-direction slicing, WAAM

Lam NGUYEN[1]
Johannes BUHL[1*]
Markus BAMBACH[1]

DECOMPOSITION ALGORITHM FOR TOOL PATH PLANNING FOR WIRE-ARC ADDITIVE MANUFACTURING

Three-axis machines are limited in the production of geometrical features in powder-bed additive manufacturing processes. In case of overhangs, support material has to be added due to the nature of the process, which causes some disadvantages. Robot-based wire-arc additive manufacturing (WAAM) is able to fabricate overhangs without adding support material. Hence, build time, waste of material, and post-processing might be reduced considerably. In order to make full use of multi-axis advantages, slicing strategies are needed. To this end, the CAD (computer-aided design) model of the part to be built is first partitioned into sub-parts, and for each sub-part, an individual build direction is identified. Path planning for these sub-parts by slicing then enables to produce the parts. This study presents a heuristic method to deal with the decomposition of CAD models and build direction identification for sub-entities. The geometric data of two adjacent slices are analyzed to construct centroidal axes. These centroidal axes are used to navigate the slicing and building processes. A case study and experiments are presented to exemplify the algorithm.

1. INTRODUCTION

Differing from conventional manufacturing processes, additive manufacturing (AM) fabricates components/parts by adding material layer-by-layer [1]. In AM variants using a powder-bed, the material is stacked layer-by-layer along the build direction. As a consequence, it is important to add physical structures to support overhang volumes. These support structures have to be removed in post-processes, which causes extra processing time and a waste of material. The powder-bed AM variants are currently also limited regarding build-up rates and build volumes [2]. AM process variants using arc and plasma welding processes (wire-arc additive manufacturing/WAAM) are hence investigated as alternative processes for building larger parts. Modern short arc technology, such as the CMT process (cold metal transfer) from Fronius [3], makes it possible to realize

[1] Brandenburg University of Technology Cottbus–Senftenberg, Dept. of Mechanical Design and Manufacturing, Cottbus, Germany
[*] E-mail: johannes.buhl@b-tu.de
DOI: 10.5604/01.3001.0010.8827

a precise material transition between the consumable wire-shaped electrode and the component to be built up in an arc welding process, which can be used for additive manufacturing. Guiding the welding torch by an industrial robot allows for 3D metal deposition with high building rates and without the restricted building space of powder-bed AM variants [4]. Slicing algorithms used for printing on powder-bed (or in general on 3-axis) machines cannot be used for efficient tool path planning for WAAM processes. The degrees of freedom of the WAAM process require adapted methods for tool path and process planning to achieve high-quality parts [5] while keeping the processing time to a minimum. For general 3D shapes, a decomposition into part features may be necessary, so that each feature can be created in optimal orientation, avoiding out-of-position welds.

This study presents a robust algorithm to decompose a CAD model into sub-parts and to determine the building direction for each sub-part to avoid out of position welding. A short overview of slicing and decomposing methods is presented in the next paragraph. Each existing method has its own limits, thus an innovative strategy is described in the subsequent section. Finally, a demonstrator part is considered to test the developed method.

2. OVERVIEW OF DECOMPOSITION AND SLICING METHODS

In AM processes, material is deposited layer-by-layer. To enable the AM process the CAD model is sliced into a set of horizontal layers. As can be seen from Fig. 1a, the slices have a constant thickness t_0. This slicing strategy is simple and can be implemented on a three-axis machine.

Complex shapes like overhang features or bridge-like shapes as shown in Fig. 1b are a challenge in AM processes. Therefore, physical support structures are added to complex shapes [6]. Support materials can be different/similar to the parts. When the system uses multi-material deposition, support materials that are dissolvable in liquids can be used [7,8]. With the aim of saving material and reducing processing time, support structures are built as scaffolding structures [9]. Another approach to deal with complex shapes is multi-directional deposition. Differing from a set of parallel 2.5D layers, this approach is able to produce a set of 3D layers, where the layer thickness is varied within each individual layer as can be seen from Fig. 1b. Thanks to multi-axis deposition complex shapes can be manufactured without using support structures.

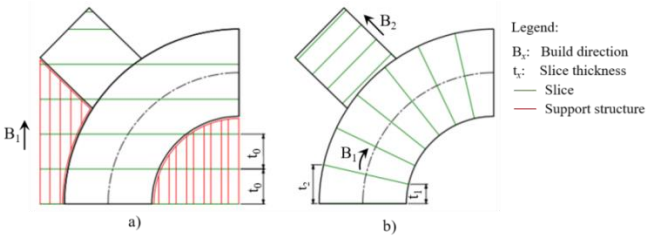

Fig. 1. Model with build direction: a) With support structures; b) Without support structures

Multi-directional deposition has attracted a great attention recently. Overhang features or bridge-like shapes are detected from a CAD model, and each feature is created with its own building direction.

Ruan et al. [10] proposed a method to vary the layer thickness and also the slicing/depositing direction. In this work, centroidal axes are established to guide the slicing and depositing processes. A normal vector is used to navigate the cutting plane. The default normal direction is the Z+ direction. Moreover, the new normal direction is computed by analyzing two adjacent layers (refer Fig. 2). The process of slicing and finding normal direction will repeat through the whole volume. At the end, centroidal axes can be defined. These centroidal axes work as a skeleton to guide the slicing and building processes.

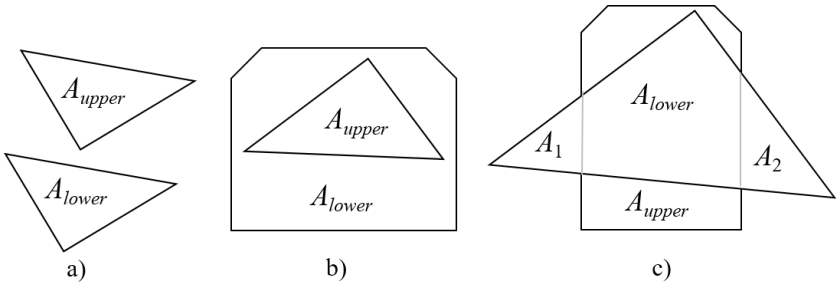

Fig. 2. The case of $\boldsymbol{A_{upper} - (A_{lower} \cap A_{upper})}$: (a) Aupper; (b) ϕ; (c) Various areas [10]

With this method, parts with curvature can be manufactured. However, it has a limit as shown in Fig. 3 [10], when this algorithm should have detected the existence of overhang features, the symmetrical overhangs are disregarded in this case, which is unreliable in real applications.

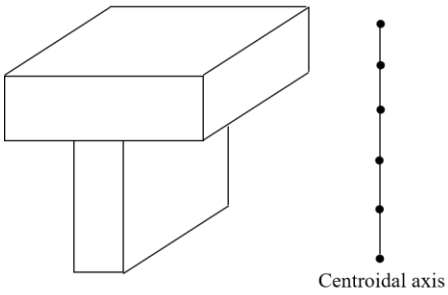

Fig. 3. Failure case for centroidal axis detection [10]

Kanakanala [6] proposed a method for detecting and slicing overhang features. Similar to Ruan et al. [10], this approach slices a CAD model with the direction of a normal vector direction. Two adjacent layers are analyzed to determine normal direction and overhangs. Let *Cb* and *Ct* denote as the centroid of bottom and top layer, respectively. The unit vector $\overrightarrow{Nb}$ is the normal vector of bottom layer and *Pb* is a point on the bottom layer which is closest to *Ct*.

$$\vec{V} = Ct - Pb \tag{1}$$

$$\gamma = (\vec{V}, \overrightarrow{Nb}) \tag{2}$$

Whenever γ exceeds a limit range, the cutting plane rotates an angle of 90° from the bottom normal vector to determine overhang features as can be seen from Fig. 4.

When the overhangs have symmetrical patterns, the normal vector $\overrightarrow{Nb}$ remains unchanged. As such symmetrical overhangs are not detected. Moreover, parts with branches (refer Fig. 5) are not considered. To be more practical, two curvature blocks should be sliced and deposited along their curvature individually.

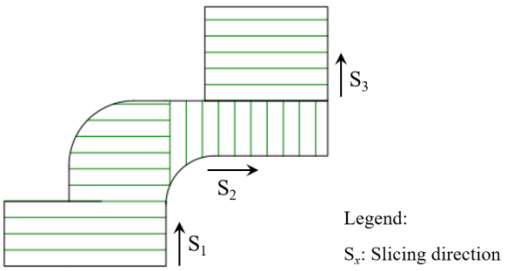

Fig. 4. Bearing seat example, as reported [11]

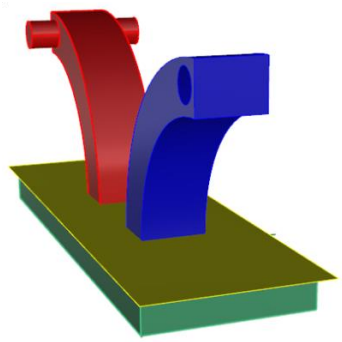

Fig. 5. An example of part with branches

Ding et al. [12] conducted research on multi-direction slicing algorithms for WAAM. Their tool consists of five main functions which are STL input, model simplification, volume decomposition-regrouping, build direction identification, and model slicing. The model simplification module is to simplify the STL file by analyzing a vast amount of triangular facets. Hole features are detected and these which are small are removed from the original model. After that, the model is decomposed into sub-volumes by using a curvature-based decomposition method. These sub-volumes have topological information which shows the sequence of manufacturing capability. In the next step, the build direction for each sub-volume is determined by a Gauss Map method [13]. Finally, each sub-volume is sliced with a certain direction.

This algorithm reveals a promising outcome for AM parts with hole features. However, it is limited since it cannot deal with complex parts which have open concave loops or non-sharp edges [12].

Lee and Jee [8] developed an extraction tool for CAD models. In this approach a cutting plane slices through a CAD model with a constant layer thickness in Z+ direction. Based on the building capability along the Z+ direction, overhang/undercut features are recognized. Overhangs/undercuts are classified as unbuildable 3D volumes. The unbuildable 3D volumes are split from the remaining buildable volumes. As a next step, the feasible part orientation is determined by rotating the positioner by 90^o. Finally, a slicing plane will slice the buildable and unbuildable volumes with a certain slicing direction.

This approach shows good results in slants along the Z axis. However, the axis of rotating and tilting can change either by 90^o or 0^o [14], as such it is not suitable for shapes with large curvatures.

The existing methods have not resolved the problems of overhangs/undercuts when parts with curvatures, branches, and symmetrical patterns are not taken into account together. Different from other existing approaches, our study presents an innovative strategy to support multi-axis slicing processes when parts with curvatures, branches, and symmetrical patterns are all considered. The CAD model is decomposed into sub-parts. For each sub-part the centroidal axis is constructed. The centroidal axis is used to navigate the cutting plane. The details of the new algorithm are explained further in the next section.

3. ALGORITHM OF CONSTRUCTING CENTROIDAL AXIS

This algorithm subdivides CAD models and establishes virtual centroidal axes for the sub-parts. The approach is to analyze the differences between two consecutive layers which are obtained by slicing the original CAD model. The slicing process is used to get data to guide the cutting plane and detect overhang features.

In this method, section curves are cross sections between a cutting plane and a CAD model. These section curves lie in a common plane, i.e. a layer. By the nature of AM processes, there is always a default layer at the bottom of AM parts. As such every layer which is created by a cutting plane from a CAD model will have a predecessor layer, here called the bottom layer and the current layer is the top layer. Each layer may contain many section curves inside. With the aim of analyzing the outer geometrical shapes between two adjacent layers, it is important to remove all section curves which encompassed by another section curve. Therefore, a *simplification module* is equipped with the aim of getting rid of inner section curves. After that, the *investigation module* is used to analyze the possible scenarios when projecting the bottom layer on the top layer. At this state, there are three possibilities such as (1) unrelated, (2) not uniform, and (3) uniform. In case (2), the cutting plane might need to change slicing direction, *normal vector identification* is adopted to track the curvature of the CAD model. In addition, when the number of centroids between two layers is different or overhangs detected, it is important to decompose/split the CAD model into sub-parts, which is accomplished in the *CAD model decomposition module*. The slicing process will result in centroids for every slice. At the end of the slicing process, an array of centroid is obtained. The *construction of centroidal axis* module uses this array to construct the centroidal axes.

3.1. SIMPLIFICATION MODULE

In order to construct the centroidal axis, only outer curves are taken into account. Therefore, it is important to remove all inner curves. This module makes the geometrical data simpler to analyze.

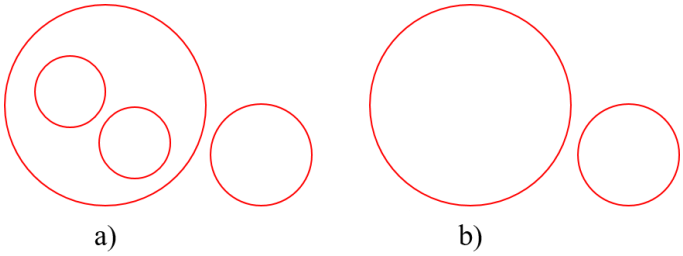

Fig. 6. Simplification: (a) Before removing inner curves, (b) After removing inner curves

3.2. INVESTIGATION MODULE

After removing all inner curves, the bottom layer is projected on the plane of the top layer. As can be seen from Fig. 7, there are four main scenarios between the projected bottom layer and the top layer. Fig. 7a reveals that two layers are not related to each other. Fig. 7c and 7d indicate that centroids *Ib* and *It* are coincident, hence the slicing direction remains unchanged. On the other hand, Fig. 7b shows differences when *Ib* and *It* are not coincident and these two layers are not uniform. In this scenario, the cutting plane might change the slicing direction, and/or slit planes are established to take off overhangs. The cutting plane changes which will be described in next section.

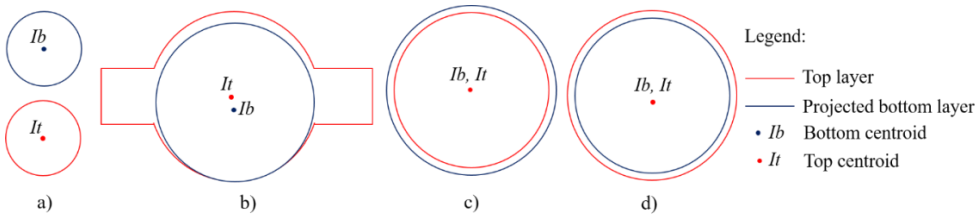

Fig. 7. Scenarios between the projected bottom and the top layer: a) Unrelated; b) Not uniform; c) & d) Uniform

3.3. NORMAL VECTOR IDENTIFICATION

Normal vector $\vec{N}$ which is always perpendicular to the cutting plane is used to navigate the cutting plane C*P* through the slicing process. The normal vector $\vec{N}$ may change when *Ib* and *It* are not coincident.

Notations:
$\vec{N}$: Normal vector
Ib: Centroid of the bottom layer
It: Centroid of the top layer
CP: Cutting plane
G: A guessed point
$\vec{V}$: Angle vector which composes by *It* and *Ib*
θ: Angle between normal vector and angle vector
α: Lower limit angle
β: Upper limit angle
h: Nominal moving distance
hmin: Minimum moving distance
hmax: Maximum moving distance
href: Moving distance reference (constant)
Initially, $\vec{N}_{init}$ is Z+ direction. The next $\vec{N}$ is equal to unit vector of $\vec{V}$.

$$\vec{V} = It - Ib \tag{3}$$

Ib of the current layer is equal to the *It* of the predecessor layer. Hence, it is vital to identify *It* by constructing a new cutting plane and then slice the CAD model. The new cutting plane goes through a guessed point *G* with $\vec{N}$ direction.

$$G = Ib + h * \vec{N} \text{ (by default } h = href) \tag{4}$$

$$\theta = (\vec{N}, \vec{V}) \tag{5}$$

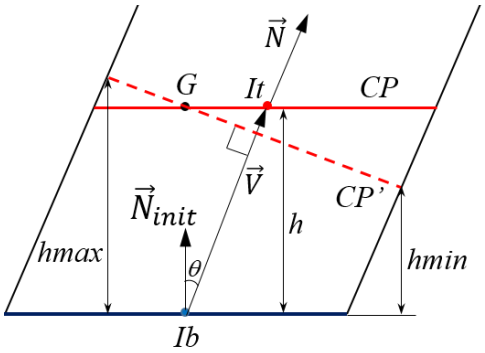

Fig. 8. Normal vector identification

If $\theta \subset [\alpha, \beta]$, the new cutting plane *CP* will be transformed. As such a new cutting plane *CP'* which is perpendicular with $\vec{V}$ is obtained as shown in Fig. 8. In some situations, the angle θ is too large. The top and bottom layer might have intersections, which is illegal. Therefore, it is important to control the nominal moving distance *h*. In this case, when h_{max} is greater than h_{ref}, a new value for *h* is computed.

$$h = \frac{hmin}{hmax} * h \tag{6}$$

The procedure of slicing and computing *It* repeats until there is no intersection between the cutting plane and the CAD model.

3.4. CAD MODEL DECOMPOSITION MODULE

A CAD model is decomposed into sub-parts when either branches or overhangs/undercuts emerge. Let *Cb* and *Ct* denote the number of outer section curves in the bottom layer and the number of outer section curves in the top layer.

Firstly, when *Ct* is larger than *Cb*, the CAD model will be split by a plane of the bottom layer. For instance in Fig. 5, the number of intersections between the slicing plane and the rectangle block is one while between the slicing plane and two curvature blocks is two; thus the value of *Cb* and *Ct* are 1 and 2, respectively. Therefore, the original CAD model is mainly decomposed into three sub-volumes.

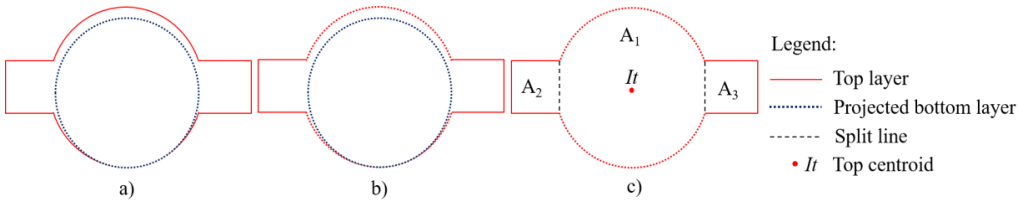

Fig. 9. Split lines determination: (a) Step 1; (b) Step 2; (c) Step 3

Secondly, when two adjacent layers are not uniform as shown in Fig. 9. Overhangs should be taken off. In this case, the projected bottom layer is divided into a set of *n* points. There will be an associated point on the top layer which is the closet point to each point on the projected bottom layer. A poly line is used to connect all those points. Those segments which have small length are considered as noises, so that they are removed. Mainly, two split lines are found and used to split the top layer into three regions A_1, A_2, and A_3. *It* just belongs to A_1. This process repeats until there is no intersection between the cutting plane and the CAD model. At the end, an array of split lines is obtained. This array is used to construct the split surfaces to decompose overhang features (refer Fig. 10c). After being taken off, these overhangs are sliced through to check whether sub-overhang features are still existing or not.

3.5. CONSTRUCTION OF CENTROIDAL AXIS

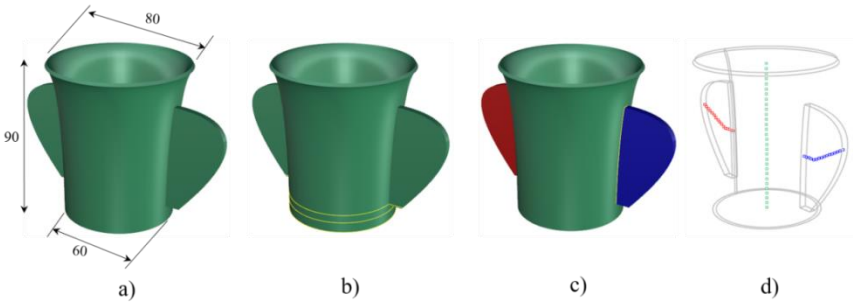

Fig. 10. Example of part decomposition: a) Solid model; b) Model slicing; c) Split overhangs; d) Centroidal axes

As can be seen from Fig. 10, the CAD model is decomposed into three sub-volumes. For each volume a centroidal axis is constructed based on *It*. For every layer *It* is computed and stored in an array. After slicing through the CAD model, these *It* points are to establish the centroidal axis.

With two settings of h_{ref} being 2 and 5 mm, the computational times are 12.86s and 8.43s, respectively. In case of curvature, the smaller h_{ref} is, the more accurately defined is the centroidal axis. However, that results in more computational time.

4. EXPERIMENTAL RESULTS

To verify the proposed method, an example of an overhang feature is developed as shown in Fig. 13, when the handles of the cup are considered as overhangs. First of all, the CAD model is sliced along the Z+ axis. At every slice, two layers are analyzed based on their geometry.

As can be seen from Fig. 9, when the bottom layer is projected on the top layer, there are some areas which are outside the top region and are thus considered as overhang features. The procedure of taking off overhangs is described in section 0. The top layer is divided into three areas which are A_1, A_2, and A_3. When A_2 and A_3 are considered as overhang area, the top layer centroid *It* is calculated on the area of A_1. It is simple when using straight lines to split the overhang areas. However, it shows some disadvantages in some cases. As can be seen from Fig. 11, when the overhang areas are large, straight split lines might intersect the inner curve. Therefore, bent curves are required when the cross-sections are annular-shaped.

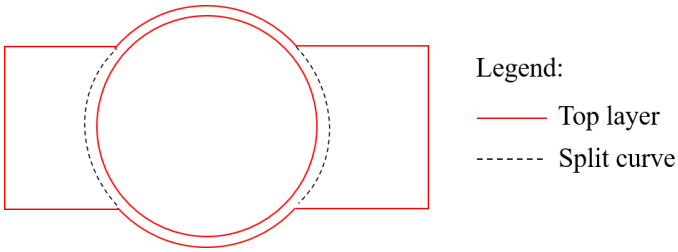

Fig. 11. An example of split curves

After slicing through, the CAD model is decomposed into three sub-parts and the centroidal axes are established as shown in Fig. 10d, respectively. When slicing the bottom of the cup, the cross-section is circle-shaped zone. Further when the cutting plane slices the cylinder, the cross-section is an annular zone. Although the areas of these two cross-sections are different, the outer curves are taken into account only as stated in section 0. Therefore, they are uniform and the cutting plane does not change the slicing direction. As such, the bottom and the cylinder are one part only. In addition, the centroidal axis of the cylinder is along the Z axis, and the centroidal axes of the handles are bent according to the centroid of each layer *It*.

In order to generate the trajectory planning for the robot as depicted in Fig. 12, three sub-parts need slicing into a set of layers with the maximum height of 1.1 mm along their centroidal axes. An in-house CAM software was develob)ped to generate the tool path for the industrial robot.

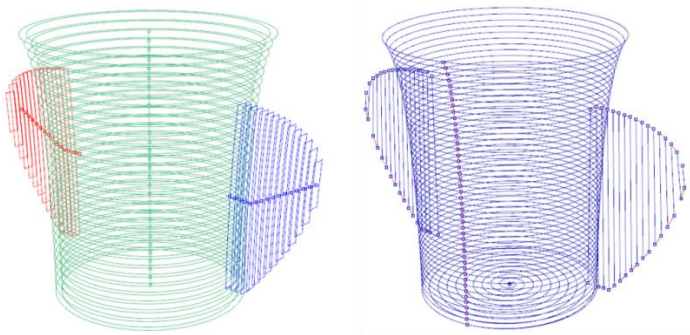

a) b)

Fig. 12. Trajectory planning: a) Slicing sub-parts; b) Tool path generation

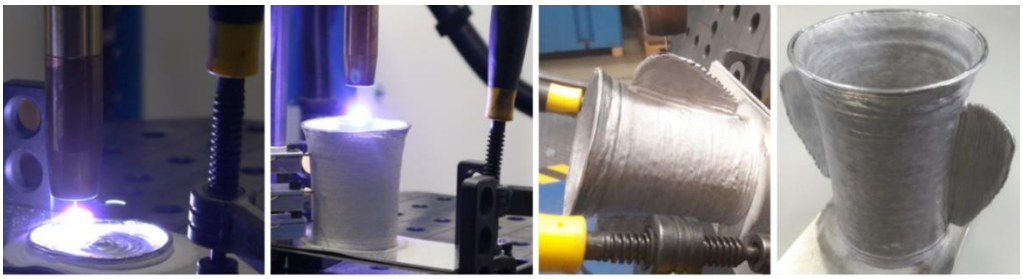

a) b) c) d)

Fig. 13. Building overhang features: a) Building the bottom; b) Building the cylinder; c) Building the handles; d) Finished part

Fig. 13 depicts the process of building the overhang features. The material which is used in this experiment is AlSi5. The hardware consists of a Fanuc 100iC robot arm equipped with a CMT feature and a rotary positioner. The shielding gas is 100 percent Argon. The bottom of the cup is first deposited and then the cylinder along its centroidal axis. Subsequently, the positioner tilts/rotates with a specific angle to deposit the handles. For each layer the robot arm and the positioner manipulate the building direction based on their centroidal axes. Thanks to that the two overhangs are built without adding support material.

5. CONCLUSIONS AND FUTURE WORK

This paper presents a first step towards a new method to deal with the problem of overhangs in wire-arc additive manufacturing. To build-up each part feature in an optimal direction, the approach of this algorithm is to decompose a CAD model into some sub-parts.

For these parts, the centroidal axis is established to guide the slicing and building processes. This centroidal axis is obtained by analyzing the geometrical information of two adjacent layers. The proposed algorithm is able to operate with symmetrical overhangs, curvatures, and branches. When it comes to symmetrical overhangs, the proposed algorithm can detect the existence of overhangs and construct centroidal axis for them.

The centroidal axis works as a skeleton of the part, which is helpful to track the cutting plane in the slicing process. The cutting plane can change the slicing direction. As such parts with curvature can be fabricated.

Moreover, the proposed algorithm can detect the existence of branches and split them. When branches have similar building direction, for example Z+ direction, the cutting plane does not need to navigate along the curvature. However, when branches are not in the same direction as shown in Fig. 5, each branch is taken into account individually. For instance, these two branches are split up from the rectangle block and then each branch is sliced through in order to construct the individual centroidal axis.

This method is not universal and might not work for all kind of geometries. Constructing the centroidal axis is based on the centroid. When layers are open curves, the centroid might not be accurate; which results in an inaccurate centroidal axis. Further improvements of this algorithm will be a complete decomposition module which can operate any complex parts, and the wire head orientation collision and gravity deposition direction problems.

REFERENCES

[1] FRAZIER W.E., 2014, *Metal additive manufacturing*, A Review, Journal of Materials Engineering and Performance, 23/6, 1917-1928.

[2] MARTINA F., MEHNEN J., WILLIAMS S. W., COLEGROVE P., WANG F., 2012, *Investigation of the benefits of plasma deposition for the additive layer manufacture of Ti–6Al–4V*, Journal of Materials Processing Technology, 6, 1377-1386.

[3] PICKIN C.G., WILLIAMS S.W., LUNT M., 2011, *Characterisation of the cold metal transfer (CMT) process and its application for low dilution cladding*, Journal of Materials Processing Technology, 3, 496-502.

[4] KAPUSTKA N., HARRIS I.D., 2014, *Exploring arc welding for additive manufacturing of titanium parts*, Welding Journal, 93/3, 32-35.

[5] WULLE F., COUPEK D., SCHÄFFNER F., VERL A., OBERHOFER F., MAIER T., 2017, *Workpiece and machine design in additive manufacturing for multi-axis fused deposition modeling*, Procedia CIRP, 60, 229-234.

[6] LIOU F., SLATTERY K., KINSELLA M., NEWKIRK J., CHOU H., LANDERS R., 2007, *Applications of a hybrid manufacturing process for fabrication of metallic structures*, Rapid Prototyping Journal, 13/4, 236-244.

[7] EUJIN P., DURAN C., SUBBIAN V., GIOVANETTI M.T., SIMKINS J.R., BEYETTE Jr,F.R., 2015, *Experimental desktop 3D printing using dual extrusion and water-soluble polyvinyl alcohol*, Rapid Prototyping Journal, 21/5, 528-534.

[8] LEFKY C.S., ZUCKER B., WRIGHT D., NASSAR A.R., SIMPSON T.W., HILDRETH O.J., 2017, *Dissolvable supports in powder bed fusion-printed stainless steel*, 3D Printing and Additive Manufacturing, 4/1, 3-11.

[9] CAI Y., 2016, *Instinctive computing*, Springer, London.

[10] RUAN J., SPARKS T.E., PANACKAL A., LIOU F.W., EIAMSA-ARD K., SLATTERY K., et al., 2007, *Automated slicing for a multiaxis metal deposition system*, Journal of Manufacturing Science and Engineering, 129/2, 303.

[11] KANAKANALA D., 2010, *Multi axis slicing for rapid prototyping*, Masters Theses 4990.

[12] DING D., PAN Z., CUIURI D., LI H., LARKIN N., Van DUIN S., 2016, *Automatic multi-direction slicing algorithms for wire based additive manufacturing*, Robotics and Computer-Integrated Manufacturing, 37, 139-150.

[13] GAN J.G., WOO T.C., TANG K., 1994, *Spherical Maps*, Their Construction, Properties, and Approximation, Journal of Mechanical Design, 116, 2/357.

[14] LEE K,. JEE H., 2015, *Slicing algorithms for multi-axis 3-D metal printing of overhangs*, Journal of Mechanical Science and Technology, 29/12, 5139-5144.